Research article

Phosphate reclaim from simulated and real eutrophic water by magnetic biochar derived from water hyacinth

Ru Cai [a], Xin Wang [a, *], Xionghui Ji [b, **], Bo Peng [a], Changyin Tan [a], Xi Huang [b]

[a] College of Resources and Environmental Science, Hunan Normal University, Changsha, Hunan, 410081, China
[b] Soil and Fertilizer Institute of Hunan Province, Ministry of Agriculture Key Lab of Agri-Environment in the Midstream of Yangtze River Plain, Changsha, 410125, China

ABSTRACT

In this study, the efficiency and mechanism of aqueous phosphate removal by magnetic biochar derived from water hyacinth (MW) were investigated. The MW pyrolyzed at 450 °C (MW450) exhibited the most prominent phosphate sorption capacity, which was estimated to be 5.07 mg g^{-1} based on Langmuir–Freundlich model. At an initial phosphorus (P) concentration of 1 mg l^{-1}, >90% P removal was achieved over pH 3–9, but the efficiency decreased sharply at pH > 10. The presence of arsenate and carbonate could remarkably decrease P sorption, while the inhibition effects of antimonate, nitrate and sulfate were less significant. In further application of MW450 to reclaim P from eutrophic lake waters (0.71–0.94 mg l^{-1} total P), ~96% P removals were attained in the batch studies and the effluent P concentrations in the column tests were reduced to <0.05 mg l^{-1} within 509–1019 empty bed volumes. As indicated by XRD, MW450 surface was dominated by Fe_3O_4 and Fe_2O_3, resulting in a good ferromagnetic property of this composite (saturation magnetization 45.8 emu g^{-1}). Based on XPS, P sorption onto MW450 occurred mainly by surface complexation with the hydroxyl *via* ligand exchange. These results highlighted that MW derived from highly damaging water hyacinth could provide a promising alternative for P removal from most eutrophic waters.

© 2016 Elsevier Ltd. All rights reserved.

1. Introduction

Phosphorus (P) is a major but the least mobile nutrient in soil and, thus, shows the lowest phytoavailability for plant growth, especially for paddy rice (Rengel and Marschner, 2005; Yadav et al., 2012). In the main rice-producing areas in southern China, successive application of a high amount of P to advance rice yield has greatly contributed to eutrophication in freshwater lakes (Guo, 2007; Duan et al., 2009; Liang et al., 2016). Moreover, the lack of efficient sewage treatment in a range of less-developed regions has exacerbated water eutrophication by allowing continuous P input into various water bodies, especially those with low flow rates. In surface water, P concentration exceeding 0.05 mg l^{-1} may cause eutrophic conditions (Hinesly and Jones, 1990). According to this criterion, a number of lakes in China are already in eutrophic state with total P up to 0.12–0.49 mg l^{-1} (Fig. S1). This is not only

threatening water quality but also aquatic biodiversity and human wellbeing (Li et al., 2008; Gong et al., 2009; Zan et al., 2011; Chen et al., 2014; Hillman et al., 2014; Wu et al., 2014). Therefore, water eutrophication has now become a major environmental and public health challenge confronting China. Developing cost-effective technologies are critical in order to trap and reclaim P from eutrophic waters.

Since the late 1960s, a variety of physicochemical and biological technologies have been established mainly for phosphate removal from municipal and industrial effluents (Onar et al., 1996; Morse et al., 1998; Yao et al., 2011a) With a minimal requirement for system operation and little addition of chemicals, P sorption using widely available and high-affinity sorbents has exhibited important potential in cost-effectiveness and environmental friendliness (Li et al., 2006; Karageorgiou et al., 2007; Hamdi and Srasra, 2012; Vasudevan and Lakshmi, 2012). Recently, a biochar derived from the residue of anaerobically digested sugar beet tailings has been shown to remove P efficiently from aqueous solutions (Yao et al., 2011a, b). In their studies, the prominent P sorption capacity of biochar was mainly attributed to the enriched MgO particles with a high point of zero charge (PZC_{MgO} = 12), which facilitated P

complexation at the hydroxylated MgO surface. In scaled-up applications, however, it could be difficult to recover the powdered biochar from the effluent. Moreover, most biochar with relatively high alkalinity (pH 7–12) and low pH_{PZC} (<4) generally has a low anion exchange capacity (<5 cmol kg^{-1}) and thus, very limited sorption capacity towards the negatively charged anions, such as P (Mohan et al., 2007; Beesley et al., 2011; Mukherjee et al., 2011; Hale et al., 2013).

To further explore the potential of biochar for efficient removal of problematic anion species, a magnetic biochar (MW) composed of iron oxides was prepared by chemical co-precipitation of Fe^{2+}/Fe^{3+} on water hyacinth biomass followed by pyrolysis. The MW exhibited a notable capability to remove aqueous arsenate [As(V)] with the used sorbents being easily separated with a magnet (Zhang et al., 2016). Phosphate and As(V) are chemical analogs with many similarities (Elias et al., 2012) and, thus, it is conceivable that this MW could be effective in P reclaim from eutrophic waters. Furthermore, water hyacinth native to South America has been identified as a highly invasive water weed with rapid growth rates and extensive dispersal capabilities, which emerged in most tropical and subtropical areas in more than 50 countries including China (Plummer, 2005; Jafari, 2010; Shanab et al., 2010; Zhang et al., 2010). Seasonal outbreak of water hyacinth in a substantial number of surface waterbodies, partially due to water eutrophication, has caused extensive environmental, economical and societal problems (Villamagna and Murphy, 2010; Patel, 2012; Zhang et al., 2015). Therefore, the conversion of water hyacinth biomass into magnetic biochar could provide a useful concept for better management of this highly problematic and invasive species.

The objectives of the present study are (1) to demonstrate the kinetics and equilibrium isotherms of P sorption by the MW; (2) to identify the effects of pH and accompanying anions on P sorption; (3) to elucidate the underlying mechanisms governing P removal; and (4) to determine P removal efficiency by the MW from actual eutrophic lake waters, which is an important but missing link to advance P reclaim by the sorption technique.

2. Materials and methods

The magnetic biochar derived from water hyacinth (MW) used in this study is an Fe oxide-biochar nanocomposite prepared according to Zhang et al. (2016) and Chen et al. (2011).

2.1. P sorption by MWs

In light of Chinese discharge standards of pollutants for municipal wastewater treatment plants (GB18918-2002), the maximum allowed threshold of P in treated municipal wastewater ranges from 1 to 5 mg l^{-1}. Moreover, the upper limit of P concentration allowed in direct discharge from the phosphate fertilizer industry is 15 mg l^{-1} according to the discharge standard of water pollutants for phosphate fertilizer industry proposed by Ministry of Environmental Protection of China (GB15580-2011). Based on the above standards, three representative P levels, i.e. 1, 5, 15 mg l^{-1}, were chosen for the following P sorption tests. P solutions were prepared by dissolving KH_2PO_4 (guaranteed reagent grade) in distilled water.

2.1.1. Experiment 1 comparison of P removal efficiency by MW250-550

To compare P removal efficiency by different MWs, 0.2 g of each MW sample was added to 40 ml of P solution containing 1 or 15 mg l^{-1} P. The no-biochar control was also included. Each treatment had at least three replicates and the initial pH of each P solution was adjusted to 7 with 1 M NaOH or 1 M HCl. The mixtures

were then subjected to mechanical agitation for 24 h at 25 ± 0.5 °C. Upon filtration through 0.22 μm filters, P concentrations in the filtrates were determined by the ammonium molybdate spectrophotometric method (GB11893-89, Ministry of Environmental Protection of China) with an ultraviolet spectrophotometer (Shimadzu, UV-2550, Japan) at wavelength 700 nm. Based on the results of this experiment, MW450 was chosen for further tests due to its higher P removal capacity.

2.1.2. Experiment 2 selection of the optimal solid/solution ratio

To identify the effect of adsorbent dose on P removal, MW450 was mixed with the P solution (1 mg l^{-1} P, pH = 7) at solid/solution (w/v) ratio from 1:100 to 1:1000. After 24 h of agitation, levels of P were determined as described above.

2.1.3. Experiment 3 sorption isotherm

The sorption isotherms of P by MW were determined by mixing 0.2 g MW450 with 40 ml P solution of different P concentrations from 0.186 to 150 mg l^{-1}. No-P and no-MW450 controls were also included. Each treatment had at least three replicates. The mixtures were adjusted to pH 7, shaken for 24 h at room temperature, and then filtered. Preliminary experiments had demonstrated that equilibrium was reached in 24 h. After this period, the suspensions were filtrated and the filtrates were used for P measurements.

2.1.4. Experiment 4 sorption kinetics

The kinetics were studied by adding 0.2 g of MW450 into 40 ml of P solutions containing 1, 5 or 15 mg P l^{-1}. The mixtures were agitated for a specified time period from 5 min to a maximum of 48 h. At each time interval, three replicates from each treatment were taken and the filtrates were analyzed for P.

2.1.5. Experiment 5 effect of pH and coexisting anions on P removal

In order to study the effects of pH on P sorption, P solutions (1, 5 and 15 mg l^{-1} P) were adjusted to pHs ranging from 3 to 12 using 1 M NaOH or 1 M HCl. Aliquots of MW450 were then added to the P solutions at varying pH and P concentrations were detected after 24 h of agitation.

The impacts of the co-existence of As(V), antimonate [Sb(V)], nitrate (NO_3^-), sulfate (SO_4^{2-}), and carbonate (HCO_3^-) on P sorption were investigated by preparing the stock solutions of these oxyanions from NaH_2AsO_4, $KSb(OH)_6$, $NaNO_3$, Na_2SO_4 and $NaHCO_3$, respectively. Aliquots (0.2 g) of MW450 were added to P solutions (initial P of 5 mg l^{-1}, i.e. 0.16 mmol l^{-1}) with single competitive anion of different concentrations from 0.15 to 0.5 mmol l^{-1}. The mixtures were shaken for 24 h. After filtration, As and Sb concentrations in the equilibrium solutions were analyzed with an atomic fluorescence spectrometer (AFS6500, Haiguang, Beijing). Aqueous NO_3^-, SO_4^{2-}, HCO_3^- concentrations were determined by the ultraviolet spectrophotometric method (Chen et al., 2011; Frenzel and Rauterberg, 1992; Mecozzi and Monakhova, 2013).

2.2. Lab-scale application of MW450 for P removal from eutrophic lake waters

Lake Dianchi located in Yunnan province is one of the most eutrophic freshwater lakes in China. Long-lasting algal blooming in this lake has drawn great attention from both public and scientific communities (Qu and Fan, 2010) concerning its degradation. In the present study, water samples were collected from three sub-areas of this lake, which differed remarkably in the eutrophication degree (Fig. 1 and Table 1). Basic chemical properties of the water samples, including pH, P, total nitrogen (TN), permanganate index (CODMn), chlorophyll a (Chl a) were assessed according to Wei (2002).
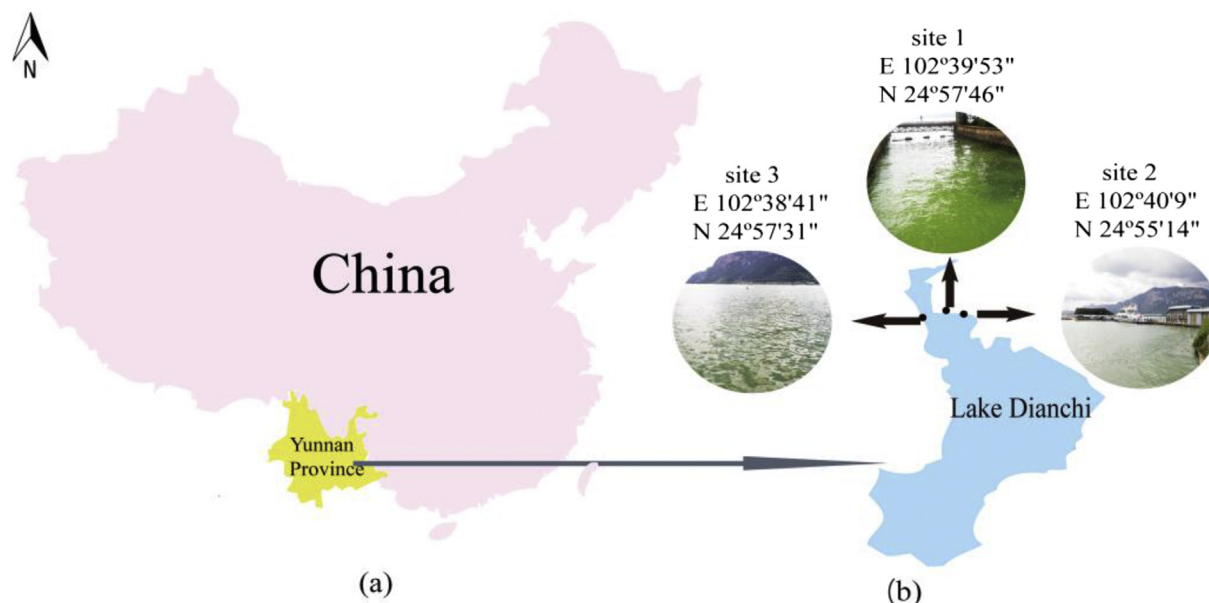
Fig. 1. The location of Lake Dianchi in China (a) and three different water sampling sites (site 1, site 2 and site 3) on Lake Dianchi (b).

Table 1
Basic background chemical characters of the eutrophic water samples from Lake Dianchi (water collection depth: 0–50 cm).

Sample	pH	TP (mg l^{-1})	TN (mg l^{-1})	COD(Mn) (mg l^{-1})	Chla (mg m^{-3})	Transparency (m)
site 1	8.54	0.94	6.32	40.17	727	0.156
site 2	8.32	0.80	5.56	38.52	523	0.212
site 3	7.91	0.71	3.52	28.88	402	0.624

2.2.1. Experiment 1 effect of MW450 dosage on P removal from the eutrophic lake waters

To determine the effects of MW450 dose on P removal from the actual eutrophic waters, the adsorbent was put into contact with the water samples at different solid/solution (w/v) ratios from 1:100 to 1:1000. After 24 h of agitation, the suspensions were filtrated through 0.22 μm filters and the aqueous P concentrations were measured by a UV spectrophotometer.

2.2.2. Experiment 2 column tests

The capacity of MW450 for P removal from the eutrophic waters was further studied with the column penetration tests. Three identical columns (200 × φ10 mm) were set up with each being packed with 1 g MW450. Empty bed contact time (EBCT) was kept at 5 min. The columns were fed by the eutrophic water samples with three different P levels at a flow rate of 0.16 ml min^{-1} by peristaltic pumps. The effluent was collected continuously in 50 ml fractions. P concentrations in the effluents were determined with a UV spectrophotometer.

2.3. Investigation of sorption mechanisms

Basic characterization of MW450 can be found in Zhang et al. (2016). To achieve a better understanding of the sorption behavior of MW450 towards P, zeta potential of the colloidal sorbent was determined in the present study. Briefly, ~0.2 g of MW450 was added to 40 ml DI water and the suspension pH was adjusted to 2–12 with 1 M HCl or 1 M NaOH. The mixtures were then shaken for 12 h at 200 rpm using a mechanical shaker followed by an ultrasonically-assisted dispersion. After filtration through 0.45 μm

filters, zeta potential of each supernatant solution was determined using a Zetasizer Nano ZS90 (Malvern, England).

To image the surface morphology and analyze the superficial element composition of this MW before and after P sorption, MW450 sample was added into 200 mg l^{-1} P solution followed by agitation for 24 h at 25 °C. The initial and post-sorption samples were then examined comparatively by scanning electron microscope (SEM, JEOL JSM-63-60LV) at 20 keV coupled with energy dispersive X-ray spectroscopy (EDX, EDX-GENES1S60S).

To further identify any formation of crystallographic minerals, samples of MW450 before and after P sorption were detected by X-ray diffraction (XRD). XRD analysis was conducted using a computer-controlled X-ray diffractometer (D/max 2500, Rigaku, Japan) equipped with a stepping motor and graphite crystal monochromator. In addition, both the pre- and post-sorption MW450 samples were subjected to X-ray photoelectron spectroscopy analysis (XPS, Thermo sher-VG Scientific ESCALAB 250Xi, USA) to determine the chemical environment of P on MW450 surface.

2.4. Statistical analysis

All results in this study were expressed as an average of three replicates with standard deviation. Treatment effect was analyzed by one-way analysis of variance (ANOVA) and significant differences at $p < 0.05$ level were determined by Student's t-test (SPSS 19.0). Kinetic and isotherm models were employed to fit the P sorption data in Origin 9.

3. Results and discussion

3.1. Effects of Fe loading, pyrolysis temperature and solid/solution ratio on P removal

0–22.8% and 0–37.7% reductions in P concentration were observed for the water hyacinth biochar without Fe loading at initial P of 1 and 15 mg l^{-1} (Fig. S2), respectively. In contrast, significantly improved P sorption capacity was recorded with MWs after Fe loading (Fig. S2). For example, aqueous P concentrations after 24 h equilibration with MWs were reduced by 77–100% and
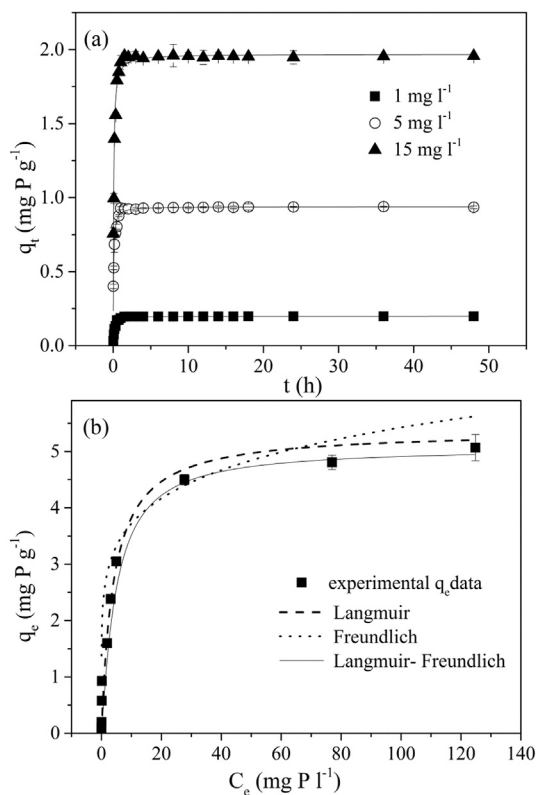
Fig. 2. Sorption kinetics data and pseudo-second-order modeling (a) and isotherm data and modeling (b) for P onto MW450 (pH = 7, T = 25 ± 0.5 °C, and sorbent concentration of 5 g l^{-1}).

25.7—81.3% at initial P of 1 and 15 mg l^{-1}, respectively. In comparison, MW450 exhibited 21—44 fold higher P sorption efficiency than other MWs at initial P of 1 and 15 mg l^{-1}. Therefore, MW450 was selected for the rest of the study. MW450 had a BET surface area of 37.2 m^2 g^{-1} and a particle diameter of 161.1 nm. More physical characters of MW450 can be found in Zhang et al. (2016).

P removal as a function of the sorbent concentration is presented in Fig. S3. With the increase of MW450 dosage from 1 to 5 g l^{-1} the percent of P eliminationrose rapidly to reach a plateau of 99.2% at initial P of 1 mg l^{-1}. Further increase of MW450 mass yielded little decrease of aqueous P concentration. Based on this result, MW450/P solution was held at 1:200 in all the subsequent experiments unless otherwise specified.

3.2. Sorption kinetics and isotherms

Kinetic investigation demonstrated that P sorption onto MW450 was quite rapid. Typically, 88% of the ultimate adsorption occurred within the first 2 h and an apparent equilibrium was reached in 4 h at initial P concentration of 1, 5 and 15 mg l^{-1} (Fig. 2a). The first-order and second-order kinetic models were used to fit the experimental data and the best-fit parameters were listed in Table 2. In spite of comparable correlation coefficients ($R^2 > 0.98$) at initial P of 1 mg l^{-1}, the second-order kinetic model fitted the sorption data slightly better than the first-order kinetics at higher P levels (5 and 15 mg l^{-1}). This suggests the rate-limiting step could be a chemical sorption between P and MW450 (Mohan et al., 2007).

The Langmuir, Freundlich and Langmuir—Freundlich equations were employed to simulate the experimental isotherms (Fig. 2b). The Langmuir-Freundlich isotherm, which describes the equilibrium on both homogeneous and heterogeneous surfaces and can be applied at both low and high adsorbate concentrations, yielded a better fit to the experimental data as demonstrated by the relatively higher regression coefficient (Table 3). Moreover, the theoretical adsorption capacity derived from the Langmuir-Freundlich isotherm (5.068 mg P g^{-1}) exhibited a high agreement with the experimental data (5.128 mg P g^{-1}) (Fig. 1b). The maximum P sorption capacity of MW450 was remarkably higher than the previously reported magnetic orange peel biochar prepared with similar procedure (Q_{max} 1.24 mg P g^{-1}) (Chen et al., 2013). This difference could be partially resulted from the varying nature of the feedstocks used in different works, which may lead to differential Fe loading density. A more integrated comparison (Table 4) further suggested that P sorption capacity of MW450 was higher than a range of low-cost sorbents. Although the maximum capacity of P adsorption by MW450 was relatively lower than that of the biochar reported by Yao et al. (2011b), ~100% P can be rapidly removed by MW450 within 2 h at initial P of 1—5 mg l^{-1}. This result indicated that MW450 could be qualified to treat most eutrophic lake waters in nature. Moreover, MW450 can be recovered by its strong magnetism (45.8 emu g^{-1}, Fig. S4) from the treated water without further energy demand.

3.3. Effects of pH and coexisting anions on P removal

As shown in Fig. 3a, P removal efficiency by MW450 was little affected with initial solution pH ranging from 2 to 9 and kept ≥90% at initial P concentration of 1—15 mg l^{-1}. In particular, up to 98% P elimination was achieved at pH 2, which could result from a more positively charged MW450 surface at lower pH as the zeta potential curve of this sorbent showed as a function of pH (Fig. 3b). When the solution pH increased to 10, P elimination by MW450 was decreased to 80.4—85.4%. And a more sharp decline of P removal to 41.6—56.1% was observed when the solution pH was further raised to 11—12, which corresponded to the significant decrease of the zeta potential of MW450 (Fig. 3b). The above results suggest that P sorption onto MW450 be markedly slowed at pH > 10 due to the increased electrostatic repulsions between the sharply elevated negative surface charge and the increasingly multivalent P oxyanions ($pKa_2 = 7.21$, $pKa_3 = 12.67$) in solution. Considering most natural eutrophic waters with pH from 7 to 9 and P < 1 mg l^{-1}, MW450 could have a wide applicability for P reclaim from a majority of eutrophic water bodies.

As(V) and Sb(V) are typical chemical analogs of phosphate and have been identified as major heavy metal contaminants in a range of mining-affected areas (Bienert et al., 2008; Williams et al., 2009;

Table 2
Parameters of Pseudo-first-order and Pseudo-second-order kinetics for P sorption by MW450.

Initial P (mg l^{-1})		1	5	15
Pseudo first-order	K_1 (h^{-1})	4.469	0.913	8.482
	q_e (mg g^{-1})	0.195	1.035	1.925
	R^2	0.967	0.757	0.84
Pseudo second-order	K_2 (g mg h^{-1})	40.037	22.803	8.765
	q_e (mg g^{-1})	0.201	0.933	1.964
	R^2	0.982	0.960	0.949

Table 3
Parameters of P sorption by MW450 deduced from Langmuir, Freundlich and Langmuir-Freundlich models.

	Parameter 1	Parameter 2	Parameter 3	R^2
Langmuir	$K_L = 0.247$	$q_m = 5.370$		0.960
Freundlich	$K_F = 2.550$		$n = 6.100$	0.965
Langmuir-Freundlich	$K_{LF} = 0.165$	$q_m = 5.068$	$n = 1.13635$	0.976

Table 4
Comparison of the maximum P sorption capacity of a range of sorbents.

Sorbent	Temperature (°C)	pH range	Sorbent concentration (g l^{-1})	Q$_{max}$ (mg g^{-1})	Reference
Digested sugar beet tailing biochar	22 ± 0.5	4–6.2	2	133.1	Yao et al., 2011a
Al pillared bentonite	–	3	4	12.7	Yan et al., 2010
Magnetite Nanoparticles	room temperature	3	1	9.72	Daou et al., 2007
Activated coir-pith carbon (activated by H$_2$SO$_4$)	35	3–10	4	7.26	Kumar et al., 2010
Activated coir-pith carbon (activated by ZnCl$_2$)	35	6–10	6	5.1	Namasivayam and Sangeetha, 2004
Magnetic water hyacinth biochar	25	3–9	5	5.07	This study
Natural palygorskite	25	4–6	1	4.00	Ye et al., 2006
Dewatered alum sludge	20 ± 2	4.3–6	–	3.50	Yang et al., 2006
Montmorillon-ite	room temperature	4–5	5–6	3.20	Jiang et al., 2003
Red mud	40	2	1	0.8	Huang et al., 2008
Magnetic orange peel Biochars	25	–	6.25	0.22–1.24	Chen et al., 2011
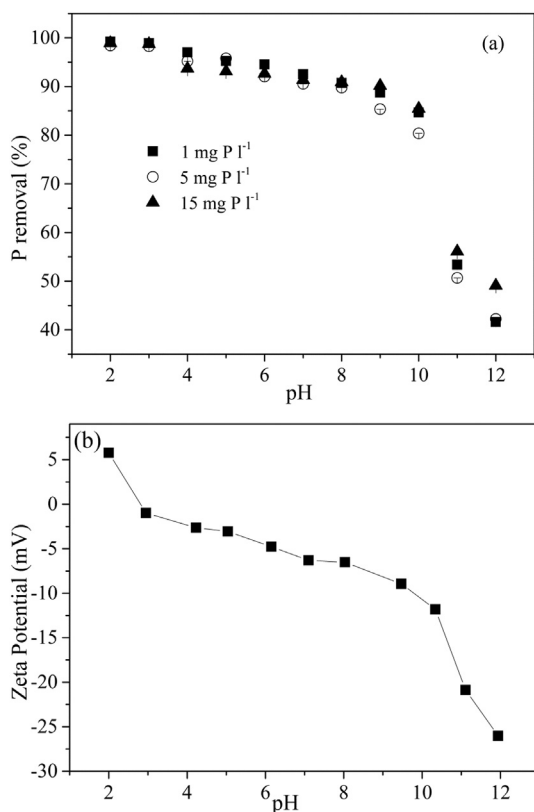
Fig. 3. Effect of pH on P removal by MW450 (a) and zeta potential of MW450 at different pH (b).

Fig. 4. P removal in the presence of different anions (a) and the concurrent removal of competitive anions (b) by MW450 (initial P = 5 mg l^{-1}, i.e. 0.16 mM, initial pH = 7).

Fu et al., 2010; Okkenhaug et al., 2012; Xu et al., 2016). As a result, the co-existence of As(V) and Sb(V) in eutrophic waters may compete with P for the limited sorption sites on MW450 surface. As shown in Fig. 4, As(V) exhibited the most prominent inhibition on P removal (initial P 0.16 mmol l^{-1}), with only 59.9–72.5% P being removed in the presence of As(V) (0.15–0.50 mmol l^{-1}) when compared to 100% P elimination in the control groups with no competitive anions. Besides, it is noteworthy that P adsorption was also remarkably decreased by 26.2–40.2% at the presence of HCO$_3^-$. In comparison, the inhibition effects of Sb(V), NO$_3^-$ and SO$_4^{2-}$ were much less under the experimental conditions. The significant competition between P and As(V) for sorption onto MW450 indicated, on one hand, a possibility of simultaneous removal of these two problematic anions from the eutrophic waters. On the other hand, however, when MW450 is employed for P reclaim from eutrophic water with simultaneous As contamination, re-release of

As back to soils could occur when the P-enriched fertilizers derived from the spent sorbents are incorporated into the farmland.

3.4. The effectiveness of MW450 on P removal from actual eutrophic waters

Lake Dianchi was hypereutrophic at the time of sampling in July 2015 (Table 1). With increased P and N levels in the eutrophic water samples, simultaneously enhanced COD and Chla with decreased transparency were determined (Table 1). As shown in Fig. S5, P removal from the eutrophic water samples increased with an increasing dose of MW450 and reached ~94% when the sorbent
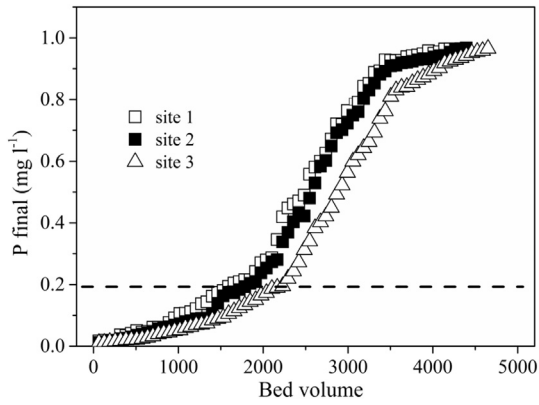
Fig. 5. P concentration in the effluent with the eutrophic water being continuous fed into the columns packed with MW450 (empty bed contact time = 5 min). Initial P concentrations in the eutrophic water from site 1, 2, and 3 were 0.94, 0.80 and 0.71 mg l^{-1}, respectively. The dotted line represents the maximum threshold of P allowed in lake and reservoir waters in China according to Chinese environmental quality standards for surface water (GB3838-2002).

concentration was increased to 5 g l^{-1}. Further increase of the MW450 mass on P removal is marginal, only 1% approaching to a maximum of 95% under the experimental condition.

In the subsequent column tests, P breakthrough behavior for MW450 was investigated with the eutrophic waters (Fig. 5). For the influent with 0.80 and 0.94 mg l^{-1} P, 5% breakthrough corresponding to ~0.05 mg l^{-1} P in the effluent which may cause eutrophic condition in surface water was not observed until 764 and 509 empty bed volume (EBV), respectively. The effluent P concentration reached 0.2 mg l^{-1} which is the maximum threshold of P allowed in lake and reservoir waters (Chinese environmental quality standards for surface water, GB3838-2002) at around 1847 EBV. The columns were exhausted at ~4000 EBV with C/C0 being higher than 95%. With lower P (0.71 mg l^{-1}) in the eutrophic water sample, the columns could treat 255 and 573 more EBV of water prior to breakthrough and exhaustion, respectively.

3.5. Sorption mechanisms

SEM-EDS analyses of MW450 before and after P adsorption were illustrated in Fig. 6. Regardless of P sorption, the SEM image of

(a)

(b)
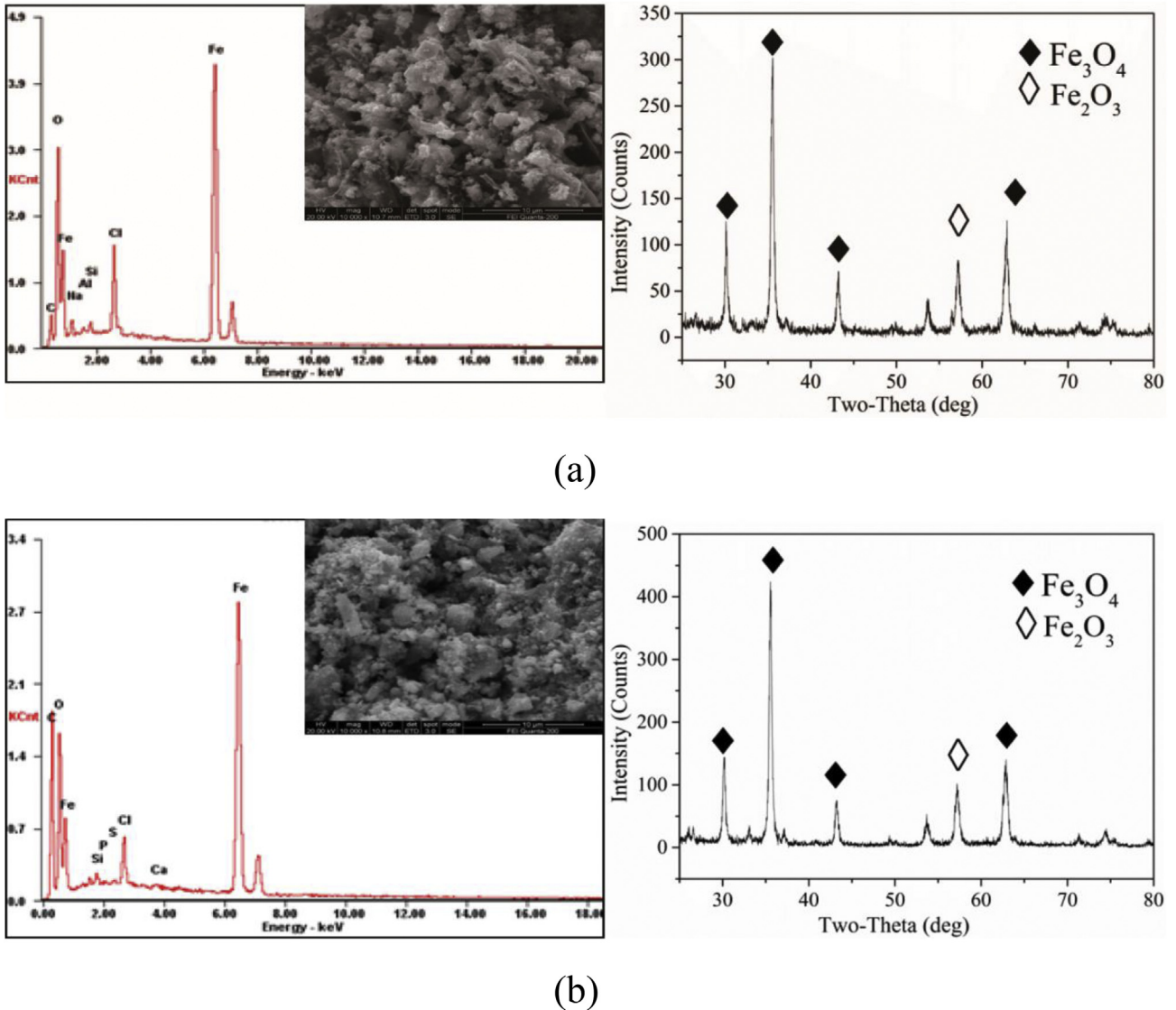
Fig. 6. SEM-EDS spectra and corresponding XRD pattern of MW 450 before (a) and after (b) P sorption.

Table 5
Fitted C1s, O1s, Fe2p3/2 and P2p3/2 peak parameters deduced from XPS spectra of MW450 before and after P sorption.

	Sample	B.E.(eV)	Assignment	Atomic content (%)
C1s	MW450	283.95	C=C	91.1
		285.34	−C−OH/C−(O)−C	8.9
	MW450 + P	283.89	C=C	86.07
		285.24	−C−OH/C−(O)−C	13.93
O1s	MW450	529.54	Fe−O−Fe	68.03
		531.54	Fe−OH	26.53
		532.39	Fe−OH$_2$	1.36
		533.08	C=O	4.08
	MW450 + P	529.34	Fe−O−Fe	47.62
		530.74	Fe−OH/Fe−O−P/P=O	30.48
		531.99	Fe−OH$_2$/P−OH	19.05
		533.29	C=O	2.85
Fe2p3/2	MW450	708.88	FeO	33.14
		710.34	Fe$_3$O$_4$	57.14
		712.59	Fe$_2$O$_3$	9.72
	MW450 + P	709.02	FeO	20.95
		710.24	Fe$_3$O$_4$	47.62
		711.69	Fe$_2$O$_3$	31.43
P2p3/2	MW450 + P	132.72	P−O/P−OH/P=O	100

MW450 surface showed evidence of mineral crystals which were mainly composed of Fe$_3$O$_4$ and Fe$_2$O$_3$ as evidenced by XRD (Fig. 6). The EDS spectra of MW450 suggested a predominance of Fe and O, accounting for 65.9% (atomic ratio) of the total surficial elements, followed by Cl and C. Compared to the initial MW450 with no P being detected by EDS (detecting limit 0.05%, mass ratio), an apparent emergence of P peak was recorded with the post-sorption sample (atomic ratio of P ≈ 0.27%), confirming P accumulation onto MW450.

For the post-sorption MW450, no peaks associated with crystal P minerals were indicated by the XRD spectra. To further identify the chemical forms of P on MW450, both the pre- and post-sorption samples were subjected to XPS analyses. The XPS wide-scan spectra of the initial MW450 showed the presence of three distinct peaks in C (C1s) at 283.95eV, O (O1s) at 529.49eV and Fe (Fe2p) at 709.75eV (Fig. S6). P sorption onto MW450 was evidenced by a P2p peak in the overall XPS spectra of the post-sorption sample (Fig. S6a). And the high resolution spectra of P2p displayed only one peak at 132.72 eV ascribed to P−O, P−OH and P=O (Daou et al., 2007). The O1s peak of the post-sorption MW450 was deconvoluted into four peaks: 529.34 eV attributed to the lattice oxygen in Fe oxide; 530.74eV to Fe−OH, Fe−O−P and P=O; 531.99 eV to P−OH and water, and 533.29 eV to C=O (Daou et al., 2007). In comparison, the relative contribution of the O1s peaks corresponding to Fe−O−P/P=O/Fe−OH and P−OH/H$_2$O increased after P sorption (Table 5). Based on these results, it is proposed that the ligand exchange between surface −OH and P anions forming Fe−O−P bond is essentially responsible for P sorption onto MW450. Besides, an apparent oxidative transformation of FeO and Fe$_3$O$_4$ to Fe$_2$O$_3$ was noticed after P sorption (Table 5), which could occur as a result of the oxidation by the dissolved oxygen in the aqueous phase during shaking.

4. Conclusions

The magnetic biochar (MW450) derived from invasive water hyacinth demonstrated a superior and constant ability for aqueous P removal from not only single-component P solution but also real eutrophic lake waters. Based on the isotherm study, the maximum P sorption capacity of MW450 was estimated to be 5.07 mg g^{-1}. P removal efficiency by MW450 was little affected over pH 3−10 while a significant inhibition of P sorption tended to occur in the

presence of comparable level of As(V), indicating that MW450 acts as a high-affinity sorbent for both P and As(V). Electrostatic attraction and surface complexation *via* ligand exchange are suggested to be the governing mechanisms controlling P sorption onto MW450.

By applying MW450 to capture P from the real eutrophic lake waters (initial P 0.71−0.94 mg l^{-1}), up to 96% of P was successfully eliminated, highlighting the potential of this sorbent in P reclaim. Scaled-up application of MW450 for minimizing P in surface waters has at least three advantages. First, particles of Fe oxides stabilized on the biochar surface through pyrolysis are more resistant to aggregation. Second, better management and control of the invasive water hyacinth could be achieved by using them as feedstocks for MW production. Third, with regard to static and intermittent sorption process, a convenient re-collection of the used sorbents would be facilitated by the strong magnetism of MW after thorough mixing of the powdered sorbents with water. Further studies may address: 1) the recycling use of bio-oil from pyrolysis as energy source to further decrease the production cost of MWs, and 2) efficient desorption of P from the spent-sorbent to produce economic P fertilizers.

Appendix A. Supplementary data

Supplementary data related to this article can be found at http://dx.doi.org/10.1016/j.jenvman.2016.11.047.

References

Beesley, L., Moreno-Jiménez, E., Gomez-Eyles, J.L., Harris, E., Robinson, B., Sizmur, T., 2011. A review of biochars' potential role in the remediation, revegetation and restoration of contaminated soils. Environ. Pollut. 159, 3269–3282.
Bienert, G.P., Schüssler, M.D., Jahn, T.P., 2008. Metalloids essential, beneficial or toxic? Major intrinsic proteins sort it out. Trends Biochem. Sci. 33, 20–26.
Chen, B., Chen, Z., Lv, S., 2011. A novel magnetic biochar efficiently sorbs organic pollutants and phosphate. Bioresour. Technol 102, 716–723.
Chen, K., Zhao, K., Zhang, H., Sun, Q., Wu, Z., Zhou, Y., Zhong, Y., Ke, F., 2013. Phosphorus removal from aqueous solutions using a synthesized adsorbent prepared from mineralized refuse and sewage sludge. Environ. Technol. 34, 1489–1496.
Chen, X., Chuan, X., Yang, X., 2014. Status quo, historical evolution and causes of eutrophication in lakes in typical lake regions of China. J. Ecol. Rural. Environ. 30, 438–443.
Daou, T.J., Begin, C.S., Greneche, J.M., Thomas, F., Derory, A., Bernhardt, P., Legare, P., Pourroy, G., 2007. Phosphate adsorption properties of magnetite-based nanoparticles. Chem. Mater. 19, 4494–4505.
Duan, H.T., Ma, R.H., Xu, X.F., Kong, F.X., Zhang, S.D., Kong, W.J., Hao, J.Y., Shang, L.L., 2009. Two-decade reconstruction of algal blooms in China's Lake Taihu. Environ. Sci. Technol. 43, 3522–3528.
Elias, M., Wellner, A., Goldin-Azulay, K., Chabriere, E., Vorholt, J.A., Erb, T.J., Tawfik, D.S., 2012. The molecular basis of phosphate discrimination in arsenate-rich environments. Nature 491, 134–137.
Frenzel, W., Rauterberg, A., 1992. High speed determination of sulfate by nonsuppressed ion chromatography. Microchim. Acta 106, 175–182.
Fu, Z., Wu, F., Amarasiriwardena, D., Mo, C., Liu, B., Zhu, J., Deng, Q., Liao, H., 2010. Antimony, arsenic and mercury in the aquatic environment and fish in a large antimony mining area in Hunan, China. Sci. Total Environ. 408, 3403–3410.

Gong, Z.J., Li, Y.L., Shen, J., Xie, P., 2009. Diatom community succession in the recent history of a eutrophic Yunnan Plateau lake, Lake Dianchi, in subtropical China. Limnology 10, 247—253.

Guo, L., 2007. Doing battle with the green monster of Taihu Lake. Science 317, 1166—1166.

Hale, S.E., Alling, V., Martinsen, V., Mulder, J., Breedveld, G.D., Cornelissen, G., 2013. The sorption and desorption of phosphate-P, ammonium-N and nitrate-N in cacao shell and corn cob biochars. Chemosphere 91, 1612—1619.

Hamdi, N., Srasra, E., 2012. Removal of phosphate ions from aqueous solution using Tunisian clays minerals and synthetic zeolite. J. Environ. Sci. 24, 617—623.

Hillman, A.L., Yu, J., Abbott, M.B., Cooke, C.A., Bain, D.J., Steinman, B.A., 2014. Rapid environmental change during dynastic transitions in Yunnan Province, China. Quat. Sci. Rev. 98, 24—32.

Hinesly, T.D., Jones, R.L., 1990. Phosphorus in waters from sewage sludge amended lysimeters. Environ. Pollut. 65, 293—309.

Huang, W.W., Wang, S.B., Zhu, Z.H., Li, L., Yao, X.D., Rudolph, V., Haghseresht, F., 2008. Phosphate removal from wastewater using red mud. J. Hazard. Mater. 158, 35—42.

Jafari, N., 2010. Ecological and socio-economic utilization of water hyacinth (Eichhornia crassipes Mart Solms). J. Appl. Sci. Environ. Manag. 14, 43—49.

Jiang, H., Liao, L.B., Wang, S.P., 2003. Phosphate and fluoride adsorption on to hydroxy-Fe-montmorillonite complex. Geochimica 32, 573—581.

Karageorgiou, K., Paschalis, M., Anastassakis, G.N., 2007. Removal of phosphate species from solution by adsorption onto calcite used as natural adsorbent. J. Hazard. Mater. 139, 447—452.

Kumar, P., Sudha, S., Chand, S., Srivastava, V.C., 2010. Phosphate removal from aqueous solution using coir-pith activated carbon. Sep. Sci. Technol. 45, 1463—1470.

Li, Y., Liu, C., Luan, Z., Peng, X., Zhu, C., Chen, Z., Zhang, Z., Fan, J., Jia, Z., 2006. Phosphate removal from aqueous solutions using raw and activated red mud and fly ash. J. Hazard. Mater. 137, 374—383.

Li, L., Li, Y., Biswas, D.K., Nian, Y., Jiang, G., 2008. Potential of constructed wetlands in treating the eutrophic water: evidence from Taihu Lake of China. Bioresour. Technol. 99, 1656—1663.

Liang, X., Wang, Z., Zhang, Y., Zhu, C., Lin, L., Xu, L., 2016. No-tillage effects on N and P exports across a rice-planted watershed. Environ. Sci. Pollut. R. 23, 8598—8609.

Mecozzi, M., Monakhova, Y., 2013. Application of multivariate methods in the monitoring of marine environment: simultaneous determination of bromide, bicarbonate, nitrate and sulphide in seawater by ultraviolet spectroscopy. Int. J. Environ. Health 6, 235—251.

Mohan, D., Pittman, J.C.U., Bricka, M., Smith, F., Yancey, B., Mohammad, J., Steele, P.H., Alexandre-Franco, M.F., Gómez-Serrano, V., Gong, H., 2007. Sorption of arsenic, cadmium, and lead by chars produced from fast pyrolysis of wood and bark during bio-oil production. J. Colloid Interface Sci. 310, 57—73.

Morse, G.K., Brett, S.W., Guy, J.A., Lester, J.N., 1998. Review: phosphorus removal and recovery technologies. Sci. Total Environ. 212, 69—81.

Mukherjee, A., Zimmerman, A.R., Harris, W., 2011. Surface chemistry variations among a series of laboratory-produced biochars. Geoderma 163, 247—255.

Namasivayam, C., Sangeetha, D., 2004. Equilibrium and kinetic studies of adsorption of phosphate onto $ZnCl_2$ activated coir pith carbon. J. Colloid. Interface. Sci. 280, 359—365.

Okkenhaug, G., Zhu, Y., He, J., Li, X., Luo, L., Mulder, J., 2012. Antimony (Sb) and arsenic (As) in Sb mining impacted paddy soil from Xikuangshan, China: differences in mechanisms controlling soil sequestration and uptake in rice. Environ. Sci. Technol. 46, 3155—3162.

Onar, A.N., Balkaya, N., Akyuz, T., 1996. Phosphate removal by adsorption. Env. Tech. 17, 207—213.

Patel, S., 2012. Threats, management and envisaged utilizations of aquatic weed Eichhornia crassipes: an overview. Rev. Environ. Sci. Bio 11, 249—259.

Plummer, M.L., 2005. Impact of invasive water hyacinth (Eichhornia crassipes) on snail hosts of schistosomiasis in Lake Victoria, East Africa. Eco. Health 2, 81—86.

Qu, J., Fan, M., 2010. The current state of water quality and technology development for water pollution control in China. Crit. Rev. Env. Sci. Tec. 40, 519—560.

Rengel, Z., Marschner, P., 2005. Nutrient availability and management in the rhizosphere: exploiting genotypic differences. New. Phytol. 168, 305—312.

Shanab, S.M., Shalaby, E.A., Lightfoot, D.A., El-Shemy, H.A., 2010. Allelopathic effects of water hyacinth [Eichhornia crassipes]. PLos One 5, e13200.

Vasudevan, S., Lakshmi, J., 2012. The adsorption of phosphate by graphene from aqueous solution. RSC. Adv. 2, 5234—5242.

Villamagna, A., Murphy, B., 2010. Ecological and socio-economic impacts of invasive water hyacinth (Eichhornia crassipes): a review. Freshw. Biol. 55, 282—298.

Wei, F.S., 2002. Monitoring and Analysis Methods of Water and Wastewater, fourth ed. Chinese Environmental Science Publishment, China.

Williams, P.N., Lei, M., Sun, G., Huang, Q., Lu, Y., Deacon, C., Meharg, A.A., Zhu, Y.G., 2009. Occurrence and partitioning of cadmium, arsenic and lead in mine impacted paddy rice: Hunan, China. Environ. Sci. Technol. 43, 637—642.

Wu, J., Liu, W., Zeng, H., Ma, L., Bai, R., 2014. Water quantity and quality of Six lakes in the arid Xinjiang Region, NW China. Environ. Proc. 1, 115—125.

Xu, C., Zhang, B., Zhu, L., Lin, S., Sun, X.P., Jiang, Z., Tratnyek, P.G., 2016. Sequestration of antimonite by zerovalent iron: using weak magnetic field effects to enhance performance and characterize reaction mechanisms. Environ. Sci. Technol. 50, 1483—1491.

Yadav, R.S., Meena, S.C., Patel, S.I., Patel, K.I., Akhtar, M.S., Yadav, B.K., Panwar, J., 2012. Bioavailability of Soil P for Plant Nutrition. Farming for Food and Water Security, Sustainable Agriculture Reviews 10. Springer, Dordrecht, pp. 177—200.

Yan, L.G., Xu, Y.Y., Yu, H.Q., Xin, X.D., Wei, Q., Du, B., 2010. Adsorption of phosphate from aqueous solution by hydroxy-aluminum, hydroxy-iron and hydroxy-iron—aluminum pillared bentonites. J. Hazard. Mater. 179, 244—250.

Yang, Y., Zhao, Y.Q., Babatunde, A.O., Wang, L., Ren, Y.X., Han, Y., 2006. Characteristics and mechanisms of phosphate adsorption on dewatered alum sludge. Sep. Purif. Technol. 51, 193—200.

Yao, Y., Gao, B., Inyang, M., Zimmerman, A.R., Cao, X., Pullammanappallil, P., Yang, L., 2011a. Removal of phosphate from aqueous solution by biochar derived from anaerobically digested sugar beet tailings. J. Hazard. Mater. 190, 501—507.

Yao, Y., Gao, B., Inyang, M., Zimmerman, A.R., Cao, X., Pullammanappallil, P., Yang, L., 2011b. Biochar derived from anaerobically digested sugar beet tailings: characterization and phosphate removal potential. Bioresour. Technol. 102, 6273—6278.

Ye, H., Chen, F., Sheng, Y., Sheng, G., Fu, J., 2006. Adsorption of phosphate from aqueous solution onto modified palygorskites. Sep. Purif. Technol. 50, 283—290.

Zan, F., Huo, S., Xi, B., Li, Q., Liao, H., Zhang, J., 2011. Phosphorus distribution in the sediments of a shallow eutrophic lake, Lake Chaohu, China. Environ. Earth. Sci. 62, 1643—1653.

Zhang, Y., Zhang, D., Barrett, S., 2010. Genetic uniformity characterises the invasive spread of water hyacinth (Eichhornia crassipes), a clonal aquatic plant. Mol. Ecol. 19, 1774—1786.

Zhang, F., Wang, X., Yin, D., Peng, B., Tan, C., Liu, Y., Tan, X., Wu, S., 2015. Efficiency and mechanisms of Cd removal from aqueous solution by biochar derived from water hyacinth (Eichornia crassipes). J. Environ. Manag. 153, 68—73.

Zhang, F., Wang, X., Ji, X., Ma, Li, 2016. Efficient arsenate removal by magnetite-modified water hyacinth biochar. Environ. Pollut. 216, 575—583.